



Seismic Vulnerability Assessment and Development of Analytical Fragility Curves for Railroads

Amir Banimahd¹ and Freydoon Arbabi^{2*}

1. PhD Candidate, International Institute of Earthquake Engineering and Seismology (IIEES), Iran

2. Professor, Structural Engineering Research Center, International Institute of Earthquake Engineering and Seismology (IIEES), Iran, *Corresponding Author; email: farbabi@mtu.edu

Received: 18/09/2012

Accepted: 18/06/2013

ABSTRACT

In a highly seismic country like Iran, safety of lifeline systems is of utmost importance. Thus, in order to develop reliable systems that can withstand severe earthquakes, railroad tracks should be properly designed and maintained. A useful tool for the assessment of structures under earthquake is fragility curves. For railroad tracks, which are designed to withstand landslides, liquefaction, etc., i.e. disasters other than earthquakes, an empirical approach is used to establish fragility curves with specific values for critical deformations. An analytical approach provides an attractive alternative and is used here. In order to make a large number of required analyses possible, a macro-element is developed and used for modeling the track system. In this model, the ballast and subgrade are represented by nonlinear springs. Fragility curves presented here are for different types of ties and roadbed properties. The results indicate that lighter ties (wood) will result in much lower seismic forces in the system than heavy (concrete) ties.

Keywords:

Fragility curve; Lifeline; Railroad; Finite Element; Vulnerability.

1. Introduction

Because of the highly-seismic nature of the country, many segments of the existing Iranian railroad network are located in seismic zones. Hence, it is important to define pre-earthquake risk mitigation strategies and post-earthquake response evaluation of tracks. Evaluation of seismic vulnerability of the system allows for an appraisal of seismic damage to existing tracks and their structures. A significant portion of these lines has been built without regards to seismic vulnerability. They may require retrofitting and better maintenance to protect them against hazards of earthquakes. Fragility curves can be used for predicting vulnerability of the railroad track and evaluating the probability of reaching a given damage level under a specific ground motion intensity. Fragility curves for railroads provide a number of advantages. They allow for estimation of time and

level of needed maintenance, evaluation of the regional seismic risks and cost analysis of retrofitting track systems for enhanced seismic resistance [1]. Two key elements of railroads in any risk analysis for major earthquakes are tracks and bridges. Investigation of seismic vulnerability has been widely considered for highway bridges. Fragility curves have been developed for such bridges, but to a much less extent for railroad bridges.

If sufficient data are on hand for major parameters of a structure such as railroad tracks, level three reliability analyses can be performed to depict the effect of each parameter on the response of the system. Level 3 is the most comprehensive type of probabilistic study. Sufficient data are not available in most cases and thus a level two or one probabilistic study is performed. For railroads, the parameters

having the most effect are ballast properties and earthquake characteristics. The variations of ballast properties are much smaller when compared to that of earthquakes. There have been various recordings of earthquakes in many regions of Iran. Fragility curves, which show the effect of the statistical variations of earthquake characteristics and magnitudes, can be helpful in assessing seismic risks and potential losses as well as the consequences of earthquakes on a given track segment. These assessments can be used for risk management decisions, retrofitting, mitigation strategies and emergency planning. A fragility function shows the probability of damage over a range of potential ground motion intensities. Failure of some old bridges in the U.S during the 1980s led to an array of approaches and methodologies for appraising the potential damage including empirical [2-4] and analytical procedures [5-6] for producing fragility curves for such structures. These led to retrofitting of the said bridges. However, little has been done for railroads in this regard, even though they are important segments of the lifeline system. Two of the limited number of studies are reported in references [7] and [8]. In another study [9], fragility curves have been produced based on observed damage to the track during earthquakes. In that study, permanent ground deformation (PGD_f) was used as intensity measure. The data used in the latter study had been collected during strong motion quakes worldwide, for different failure modes. Failure modes included fault rupture, liquefaction, landslide, rock-fall and compression/axial strain of the ground with different conditions of soil and track. Analytical methods, on the other hand, can have a wider range of application. They are based on rules deriving from the observed data and basic principles. They can be used in the absence of sufficient empirical data and can address different track types, soil conditions and hazard levels. The fragility curves developed in this paper are based on such analytical methods.

The fragility curves thus obtained are for specific types of track, soil conditions and hazard levels. The analytical model uses finite element method to simulate the rail as a generalized beam element. For investigation of the lateral motion of the track, a simple model with two degrees of freedom (lateral translation and rotation about the vertical axis) is used. For the lateral motion of the track under earthquake,

the effect of ties is considered by modeling them as lumped masses, without rotational rigidity. The ballast is modeled by discrete springs at the locations of ties. The behavior of the ballast bed is generally nonlinear [10]. In previous studies, only monotonically increasing loads on the ballast have been considered. In this investigation, the cyclic behavior of ballast is modeled in order to realistically evaluate the cyclic response of the track system during an earthquake. For a probabilistic study, sufficient data points are needed. Here, a group of earthquakes used in the SAC report [11] is used. Ten records with hazard levels 10% in 50 years in Type *D* soil, according to NEHRP [12] standard are selected. A key parameter in fragility curves is the limit state, or the level of damage to the structure. In developing fragility curves for railroads with damage due to landslides, settlements, etc. (that is, damage by disasters other than earthquakes), the permanent ground deformation is used as damage state. Such damage state is usually based on empirical data [13]. The time history analyses performed here for the selected earthquake records show that, for some cases, the permanent ground deformation at the end of the analysis may decrease while the peak ground acceleration is increased. That is, the limit state for permanent deformation is sensitive to the earthquake characteristics. Unfortunately, measured values for permanent ground deformations due to earthquakes are not available. For this reason, the fragility curves described here have been based on peak ground deformations. These fragility curves are therefore more conservative than the ones based on permanent deformations. Should measured data for permanent ground deformations due to earthquakes become available, a relationship could be established between PGA and PGD_f , the present curves can be corrected to derive fragility curves based on PGD_f . Fragility curves presented here are for standard Iranian railroads (i.e. B70 ties and UIC 54 rails).

2. Formulation and Track Property Matrices

The advent of conversion from longitudinal ties to cross-ties was a major event in the design of railroad tracks. More recent changes include the use of continuously welded rails and the so called positive fasteners. Thus, the rails and the supporting ties and fasteners respond in tandem to lateral vibrations and seismic excitations. In any dynamic analysis, the

track model must include the rails, ties, fasteners and roadbed. Modeling of the rail is a rather straight forward process. When fasteners are combined with the rail, the resulting stiffness and mass matrices are similar to those of a regular beam on elastic foundation. Because three-dimensional finite elements are rather prohibitive for modeling the volume of the roadbed, discrete equivalent springs can be used in a one-dimensional model to depict the response of the roadbed. As a result, a beam-like macro element is developed for modeling the track. The mass of the ties is incorporated by lumped masses located at their discrete locations. An energy approach is utilized in deriving the stiffness and mass matrices of the track.

3. Matrices for Finite Element Modeling

The macro-element introduced for the rail and its supporting system consists of a three dimensional beam on springs representing the stiffness of ties, fasteners and roadbed [14]. Each element has two nodes with up to seven degrees of freedom per node. Six degrees of freedom are those of three-dimensional beams and a seventh degree of freedom, the derivative of the axial rotation, can depict warping of the section. The rail deformation is assumed to remain linear. However, the behavior of the support system can be nonlinear. A major parameter in stability of the track is its lateral resistance. This resistance may vary along the length of the track. The variation can be due to decay of the ties and ballast properties, soft spots in the ballast, and varying degrees of its consolidation. Since lateral and vertical vibrations are decoupled, a number of degrees of freedom can be restricted for investigation of the lateral vibration.

Derivation of the governing equations [15] starts by considering the deformation vector, $\mathbf{U} = \{u \ v \ w\}$, denoting the displacement of an arbitrary point of the rail element. The three components of the displacement vector are functions of x , y and z and can be expressed in terms of the displacement of the centroid of the section and lateral displacements of the shear center $u = u_c - yv'_s - zw'_s$, $v = v_s - (z - z_s)\phi$, $w = w_s + (y - y_s)\phi$ where subscripts c and s refer to the centroid and shear center of the rail, and ϕ is axial rotation of the rail. y_s and z_s are the coordinates of the shear center. A prime indicates differentiation with respect to x . The non-zero components of stress and strain vector are:

$\boldsymbol{\sigma} = \{\sigma_x \tau_{xy} \tau_{xz}\}$ and $\boldsymbol{\varepsilon} = \{\varepsilon_x \varepsilon_{xy} \varepsilon_{xz}\}$. Using Green strain tensor, the strain vector takes the form:

$\boldsymbol{\varepsilon} = \{\partial u / \partial x \ \partial u / \partial y + \partial v / \partial x \ \partial u / \partial z + \partial w / \partial x\}$. In terms of the deformation vector of the rail, the strain tensor becomes:

$$\boldsymbol{\varepsilon} = \{u'_c - (y - y_s)v'_s - (z - z_s)w'_s - (z - z_s)\phi' - (y - y_s)\phi'\}.$$

The stress tensor is $\boldsymbol{\sigma} = \mathbf{E}^T \boldsymbol{\varepsilon}$ where \mathbf{E} is the elasticity matrix with the following nonzero components: $\mathbf{E}_{11} = E$, $\mathbf{E}_{22} = \mathbf{E}_{33} = G$.

E and G are Young's and shear moduli. The elastic energy of deformation of the rail is:

$$U_r = \frac{1}{2} \int_V \boldsymbol{\sigma}^T \boldsymbol{\varepsilon} dV = \frac{1}{2} \int_V \boldsymbol{\varepsilon}^T \mathbf{E} \boldsymbol{\varepsilon} dV = \frac{1}{2} \int_V S dV.$$

Using the deformation gradient vector $\mathbf{d} = \{u'_c v'_s w'_s \phi'\}$ and defining the vector \mathbf{L}_i [16] with the following nonzero components, $\mathbf{L}_1 = \{1 \ -y \ -z \ 0\}$, $(\mathbf{L}_2)_4 = -(z - z_s)$ and $(\mathbf{L}_3)_4 = y - y_s$, we have $\boldsymbol{\varepsilon} = \mathbf{L}^T \mathbf{d}$ with $\mathbf{L} = [\mathbf{L}_1 \ \mathbf{L}_2 \ \mathbf{L}_3]$ and $S = \mathbf{d}^T \mathbf{L} \mathbf{E} \mathbf{L}^T \mathbf{d}$. The deformation gradient vector can be expressed in terms of the joint displacement vector as: $\mathbf{d} = \mathbf{D} \mathbf{r}$. The joint displacement vector has the following components $\mathbf{r}^T = \{\mathbf{r}_1^T \ \mathbf{r}_2^T\}$ with $\mathbf{r}_i^T = \{u_i \ v_i \ w_i \ \phi_i\}$, $i = 1, 2$ referring to the first and second ends of the element. Matrix \mathbf{D} is given in the Appendix I. With the above definitions, the elastic energy of deformation becomes $U_r = \frac{1}{2} \mathbf{r}^T \mathbf{K}_e \mathbf{r}$, where the stiffness of the rail element is expressed as $\mathbf{K}_e = \int_V \mathbf{D}^T \mathbf{L} \mathbf{E} \mathbf{L}^T \mathbf{D} dV$.

The effect of the support system will be represented by discrete springs in the vertical, lateral, torsional and axial directions. For springs located at the ends of the element, the stiffness matrix has a diagonal form. Under deformation, the elastic energy of the springs is $U_s = \frac{1}{2} \mathbf{r}^T \mathbf{K}_s \mathbf{r}$, with the spring stiffness matrix \mathbf{K}_s as given in Appendix I.

4. Mass and Damping Matrices

Because of the distributed nature of the mass of the system, a consistent formulation is used in the derivation of the mass matrix, Figure (1). The kinetic energy of the rail element is $T = \frac{1}{2} \rho \int_V \dot{\mathbf{U}}^T \dot{\mathbf{U}} dV$. A dot indicates differentiation with respect to time. The deformation vector, \mathbf{U} can be written as $\mathbf{U} = \mathbf{Y} \mathbf{s} + \mathbf{Z} \mathbf{s}'$ where \mathbf{Y} and \mathbf{Z} are 3×4 matrices with nonzero components $\mathbf{Z}_{12} = -y$, $\mathbf{Z}_{13} = -z$, $\mathbf{Y}_{11} = \mathbf{Y}_{22} = \mathbf{Y}_{33} = 1$, $\mathbf{Y}_{24} = -(z - z_s)$, $\mathbf{Y}_{34} = -(y - y_s)$ and the displacement vector \mathbf{s} , has four components: $\mathbf{s} = \{u_c v_s w_s \phi\}$. In terms of the joint displacement vector \mathbf{r} , we have $\mathbf{s} = \mathbf{F} \mathbf{r}$. \mathbf{F}

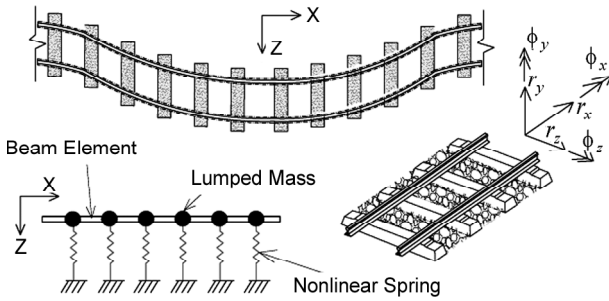


Figure 1. Simulation of the railroad track.

is the matrix of shape functions for beams, Appendix I. Thus, the kinetic energy of the rail element becomes $T = \frac{1}{2} \rho \int_V (\dot{\mathbf{r}}^T \mathbf{F}^T \mathbf{Y}^T \mathbf{Y} \mathbf{F} \dot{\mathbf{r}} + \dot{\mathbf{r}}^T \dot{\mathbf{F}}^T \mathbf{Z}^T \mathbf{Z} \mathbf{F} \dot{\mathbf{r}}) dV$. From the latter equation, we can extract the mass matrix as $\mathbf{M}_r = \rho \int_L (\mathbf{F}^T \mathbf{Q} \mathbf{F} + \dot{\mathbf{F}}^T \mathbf{I} \dot{\mathbf{F}}) dx$. Here, \mathbf{Q} and \mathbf{I} are 4×4 symmetrical matrices with nonzero components: $\mathbf{Q}_{11} = \mathbf{Q}_{22} = \mathbf{Q}_{33} = A$, $\mathbf{Q}_{44} = I_p$, $\mathbf{Q}_{24} = A z_s$, $\mathbf{Q}_{34} = -A y_s$, $\mathbf{I}_{22} = I_z$, $\mathbf{I}_{33} = I_y$, A , I_y and I_z are the cross-sectional area, area moment of inertia about y and z axes and I_p is the polar moment of inertia.

Because of their large masses, ties may cause large deformations in railways. The B70 tie has a weight of 285 kg while the UIC 54 rail weighs only 54 kg per meter (71.3 kg for a track length equal to tie spacing of 66 cm). Therefore, mass of ties is 4 times greater than that of the rails for the tributary length. For this reason, the dynamic behavior of the track cannot be accurately depicted in seismic analysis without adequately representing the mass of the ties and ballast. The damping properties of the ballast and subgrade are not well defined as to permit an accurate determination of damping factors. Thus, damping is approximated at the system level rather than from individual elements. The Rayleigh damping which is proportional to the stiffness and mass matrices is used here. In this manner, the damping matrix takes the form of $\mathbf{C} = a_0 \mathbf{M} + a_1 \mathbf{K}$, with a_0 and a_1 constants determined from two specified damping ratios at two unequal frequencies of vibration. For a simply supported uniform beam with length L resting on an elastic foundation, the frequencies can be found [17] from Eq. (1):

$$\omega_j = \sqrt{(j^4 \pi^4 EI_y + L^4 k_z) / mL^4}, \quad j = 1, 2, \dots \quad (1)$$

where E is Young's modulus, I_y moment of inertia about the y -axis, m is mass per unit length and k_z the spring constant in the z -direction. In parametric studies, we consider a 50 m track with $E = 2.1 \times 10^6$ kg/cm² and $k_z = 3540$ kg/cm. A UIC 54 rail section, commonly used in the Iranian Railroads with $I_y = 417$ cm⁴ and $m = 0.54$ kg/cm, and B70 concrete ties ($m = 280$ kg and tie spacing 66 m) are also utilized. The first 10 frequencies obtained for the model by Eq.(1) are given in Table (1) and Figure (2) along with those obtained by the finite element formulation. As we can see, the frequencies for a discretized beam on elastic foundation approaches a continuous frequency spectrum when the L/r (length/radius of gyration) ratio exceeds a threshold [17]. If two subsequent frequencies with close values are used to determine the damping matrix according to Rayleigh's method, the solution of the equations of motion for the railroad track becomes divergent. To insure the selection of two unequal frequencies, the first and the 20th frequencies are utilized in determining the values of a_0 and a_1 .

5. Nonlinear Behavior of the Track System

Under the movement of trains, especially for high-speed systems, the track is subjected to dynamic motion. Thermal loads induced by temperature change can worsen these conditions. The lateral forces induced in the track must be resisted by the

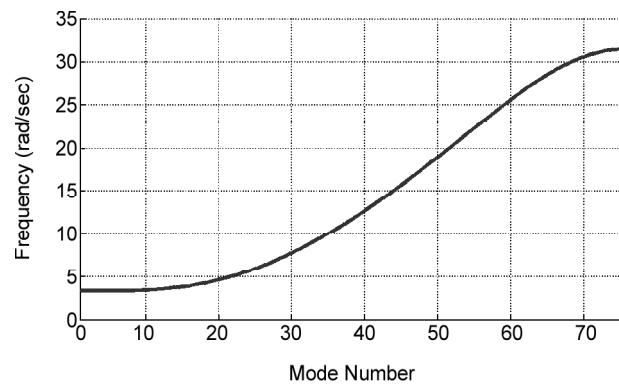


Figure 2. Frequencies of the dynamic system.

Table 1. The first 10 natural frequencies of system (rad/sec)

Mode Number (j)	1	2	3	4	5	6	7	8	9	10
Eq. (1)	3.348	3.348	3.349	3.349	3.351	3.354	3.358	3.366	3.376	3.390
Finite Element Model	3.347	3.348	3.349	3.351	3.355	3.362	3.374	3.391	3.415	3.448

lateral resistance of the track. Therefore, determination of lateral stiffness of the track is crucial in the correct evaluation of its response. At higher deflections, the resistance of the support system is nonlinear because of the nonlinear behavior of ballast. This resistance may change with type of tie and its weight, dimensions as well as ballast gradation and quality, depth of the ballast crib, its shoulder height and vertical loads. Previous investigations on lateral stiffness of the track show that the nonlinear lateral resistance of the ballast can be represented by an elasto-plastic model [10, 18, 19]. In a seismic analysis, the residual deflections of the track due to material nonlinearity must be allowed in order to determine safe operation of the line after a quake. For lateral displacement of the track, a beam on nonlinear elasto-plastic supports is commonly used. A better model that depicts the behavior of the tie-ballast system uses a tri-linear force-displacement relation, Figure (3).

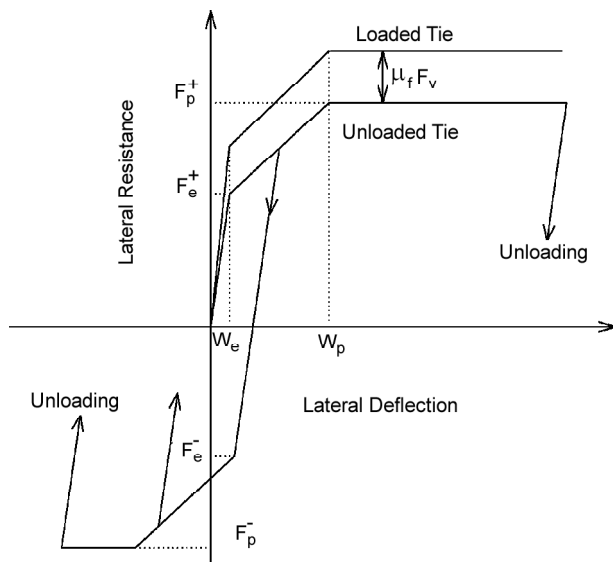


Figure 3. Dynamic resistance idealization of track.

The parameters of such a model are determined by the single tie push test. This test is usually used in the U.S. for quantifying lateral resistance of tracks [20-21]. The resistance of the track is represented by four parameters: the limit of the elastic resistance F_e , the peak resistance F_p , elastic displacement W_e , and lateral displacement of the tie at peak resistance W_p . The elastic displacement W_e is small (about 1.3 mm) and is usually ignored. The value of F_p , the peak resistance for the ballast is taken as stabilized value. This value varies between 8.9 kN and 17.8kN,

depending on the quality of ballast and its tamping condition. The limit of elastic resistance, in the absence of measured values, is taken at $F_p/4$. The effect of vertical loads is increased values of F_e and F_p . The increase is $\mu_f R_v$, Figure (3), where μ_f is the tie-ballast friction coefficient with values 0.7 and 1.0 for concrete and wood ties, respectively, and R_v is the vertical reaction force caused by the vertical wheel load. Since the weight of the train is much larger than that of the track, it can produce significant deformations in the track. The weight of train is being considered in a study to be reported in a later article. However, since the probability of a train being present on a given segment of the track when earthquake hits is very low, the results of this paper, which include unloaded tracks are only relevant to unloaded tracks.

The changing direction of an earthquake motion causes the nonlinear material to dissipate energy during each cycle. The extent of this energy dissipation is proportional to the area under the force-displacement diagram, Figure (3).

The nonlinearity of the track may be modeled by assuming a definite yield point for the support, beyond which additional displacements take place at no additional restoring force. This elasto-plastic behavior can involve unloading, reversed loading, as well as hardening of the resisting materials. From the hardening rules, i.e. isotropic, kinematic and independent, kinematic type appears to best describe the behavior of the resisting elements of the track. With this hardening rule, the elastic range is the same for loading and unloading. After the first nonlinear deformation, the ballast is no longer virgin, and its initial condition is changed. That is, after the first passage of train (first loading and unloading loop) the consolidation of the ballast changes.

An important part of the lateral resisting system in railroad tracks is rail fasteners. Fasteners allow proper positioning of rails for smooth running of trains. Modern fasteners, such as rail clips, provide varying degrees of rigidity, while older types (spike and bolt) allow little or no rigidity against rotation about the vertical axis. A simple model for investigating the lateral deflection of the track can be obtained by combining the two rails into one. For the model under consideration, the moment of inertia in the lateral direction can be expressed as $2(I_y + \kappa Ad^2)$, where A is the cross-sectional area of one rail and I_y its moment of inertia about the vertical axis, d is

half-distance between the two rails. The parameter κ equals zero when fasteners provide no rigidity and equals 1 for complete rigidity. For fasteners with partial rigidity, the stiffness is obtained by test and a general solution, such as finite element method can be used.

6. Ground Motion Records and Solution Process

Various researchers have presented a variety of earthquake records [22-23] for developing fragility curves using nonlinear time history analyses. One of the significant studies has been done under the SAC project [11], in which a group of time history records with seismic hazard levels of 10% in 50 years has been used along with the procedure suggested by McGuire [12]. The records have been classified according to the magnitude and distance from the source. Those records are used in the present study. Because many regions of Iran are seismically active, its railway network naturally passes through such high risk zones. Therefore, it is essential to consider the effects of ground motion on railway lines crossing these zones. It would be ideal to have earthquake records at moderate distances from the sources (faults) as well. However, the more common far field earthquake records are used here, which avoid directivity pulse-type effects. The procedure used for the selection of earthquake records is that described in the SAC report for hazard level of 10% probability of exceedance in 50 years and at sites located on hard soil (Type D, NEHRP). The selected ground motions are normalized at different PGA levels of up to 2 g.

Nonlinear time history analyses are performed using a step-by-step integration procedure. The Wilson- θ method is utilized because it provides a more stable solution technique than the Newmark- β and other schemes. As for the nonlinear behavior of the support system, a tri-linear curve (an elasto-plastic procedure with hardening prior to rigid plastic deformation) is used. The equation of motion of railway track has a form similar to that of other structures under earthquake, i.e. $\mathbf{M}\ddot{\mathbf{y}} + \mathbf{C}\dot{\mathbf{y}} + \mathbf{K}\mathbf{y} = -\mathbf{M}\ddot{\mathbf{y}}_g$:

The mass of springs in the lateral direction is assumed to be negligible. Thus, the mass matrix has the form: $\mathbf{M} = \mathbf{M}_{rail} + \mathbf{M}_{tie}$. Moreover, the axial stiffness of the tie is assumed to be very large compared with that of the supports (springs) in the lateral direction. The stiffness matrix can be written as: $\mathbf{K} = \mathbf{K}_{rail} + \mathbf{K}_{spring}$.

7. Fragility Curves

The progresses in methods of analysis and faster computers have made it possible to include the probabilistic nature of many of the structural parameters. One such parameter in design is the random nature of earthquakes. Compared to the variation of the properties of structures variation in potential earthquakes is a lot more severe. The search for inclusion of seismic variations by a method that is general enough and yet easy to use has led to fragility curves. Fragility curves relate the probability of failure of the structure to the peak ground accelerations of earthquake that could occur in a region [24]. The level of shaking can of course be quantified using a variety of earthquake parameters such as peak ground acceleration, velocity, displacement, permanent ground deformation, spectral acceleration, spectral velocity or spectral displacement. Fragility defines the conditional probability of the seismic demand (D) placed upon a structure exceeding its capacity (C) for a given seismic intensity level of a specific earthquake parameter (IM) i.e. $P_f = P[D \geq C | IM]$. Studies by Cornell et al [25] have indicated that for buildings fragility curves expressed by a lognormal probability, distribution function will lead to better results. In this case

$$P_f = P[d_s \geq d_{si} | IM] = \Phi(\ln(S/S_{mi})/\beta_{D|IM}) \quad (2)$$

where $\Phi()$ is the probability of exceeding a particular damage state, d_s . d_{si} is specified i^{th} damage state, S_{mi} is the median value of the seismic demand and S is its value at a given intensity level and $\beta_{D|IM}$ the logarithmic standard deviation of a given seismic intensity level defined by the earthquake parameter, IM . The value $\beta_{D|IM}$ is estimated by regression analysis.

A review of existing fragility functions is given in Ref [26] for various parts of railroad systems, such as railroad tracks, bridges and tunnels. Different approaches can be used in determining fragility curves such as empirical, judgmental, analytical and hybrid. The latter report has used an empirical approach for railroad tracks. In that, empirical fragility curves have been generated based on past earthquakes. If a set of post-earthquake data covering a wide range of ground motions and soil types is available, fragility curves can be obtained in an empirical fashion. However, only limited data for strong motion earthquakes are available, and schemes must be

devised to generate additional data. One such procedure is obtained by assuming a distribution function based on the available values or by physical principles. In this paper, an analytical approach is used to generate fragility curves, with a specific damage criterion. Because lateral displacement is the common cause of damage and derailment, fragility curves presented in this paper are for that situation.

8. Intensity Measures (IM) and Limit State

Characterization of strong ground motion quakes is a key step in seismic risk analysis of structures and lifeline networks [26]. The main issue in the selection of an appropriate earthquake intensity parameter is how it can capture the response of the structure with a minimum dispersion. The same applies to the derivation of fragility curves. Thus, empirical curves relating the observed damage to seismic intensity describe the situation better if they are based on actual records of seismic motions. It is common to base the vulnerability assessment of a wide network under ground shaking on *PGA* values. The same procedure is used in this paper. On the other hand, permanent deformations (PGD_p) are more suitable intensity measures for the study of railroads subjected to ground failures such as liquefactions, fault ruptures and landslides. Because of a lack of damage state criterion for railway elements, damage states utilized for components of roadways with similar responses are used for describing railways [27]. Limit values given in Table (2) are used to determine the damages induced as permanent ground deformations (PGD_p) [28] based on the European Standards for Track Geometric Quality. These are for failures other than those caused by earthquakes.

9. Results

Since the methods of earthquake analysis and design proposed by Housner [29] and Newmark [30] in the 1950's, the process has seen many variations. Because the earthquakes occurring in a given region appear to have some similarities, Housner suggested the average of the available records for that region to be used for the analysis. A similar procedure was used by Newmark for design in which the records of a region were averaged and simplified into a spectral curve.

In developing fragility curves, the random nature of records is taken into account by using a sufficient number (10-20) of available records. The randomness in the intensity is considered by varying the peak ground motion over a probable range. Variations in material properties and geometry are also random, but their change is much less severe as compared to that of earthquakes. Therefore, the latter variations are usually ignored in developing fragility curves.

To setup fragility curves, nonlinear time history analyses are performed for a series of earthquake records to obtain a reliable estimate of the probability of damage. For railroad tracks, the absolute maximum deformation of the line is determined for each earthquake record. A set of 10 records is used here. By fitting a power regression line to the data, the pertinent parameters are obtained. A log-normal distribution is assumed for earthquake records and the limit state is taken as the maximum deformation of the track for all failure modes. As mentioned before, this limit state is more severe than that of residual deformations. Therefore, the results yield conservative fragility curves. The analyses are performed by a code developed in Matlab medium. This code is

Table 2. Railway tracks damage state classification.

Serviceability and Repairs Required	Damage States	Direct Damages	Lateral Permanent Deformation (cm)		
			Min	Max	Mean
Closed to traffic. Replacement of track's segments is required. Duration of closure depends on length of damaged lines.	Extensive/ Complete ds_3	Major differential settlement of the ground resulting in potential derailment over extended length	10	30	20
Closed to traffic. Local repairs or replacement of tracks is required	Moderate ds_2	Considerable derailment due to differential settlement or offset of the ground.	5	10	8
Operational after inspection or short repairs.	Minor ds_1	Minor (localized) derailment due to slight differential settlement of embankment or offset of the ground.	1	5	3
Fully open to traffic	None ds_0	None	0	1	0.5

validated by a model on Structural Analysis Program (SAP) [31], see Figure (4).

Figures (6) and (7) show fragility curves for concrete and wood ties for four damage states. The weights of concrete and wood ties are 285 and 80 kg, respectively. These are the common types of ties used in the Iranian railroad system. As seen from Figures (6) and (7), wood ties induce less deformation and force under earthquake. This is somewhat akin to the situation in buildings where a reduction of mass of the floors results in a reduction of earthquake forces. In these figures, three types of springs with different yield limits are utilized, but the yield level does not seem to have any effect on the response.

Under static loads, it is obvious that the maximum deflection is inversely related to the stiffness. However, in the dynamic case and under seismic loading, the results are different. This is because of the negligible effect of the reaction force of the nonlinear spring in the equilibrium equation of the track as compared to the inertia force, Figure (5). Figure (8) shows the ratio of the maximum lateral deflection of the track to the maximum deflection at

PGA = 0.1 g. In addition, as the peak ground acceleration increases, the reaction of the springs is decreased while the inertia force has most effect on the maximum deflection. Therefore, when the resistance of the ballast is doubled, i.e. the condition of the ballast is changed from poor to good; the maximum deflection is not affected by the plastic limit of nonlinear springs.

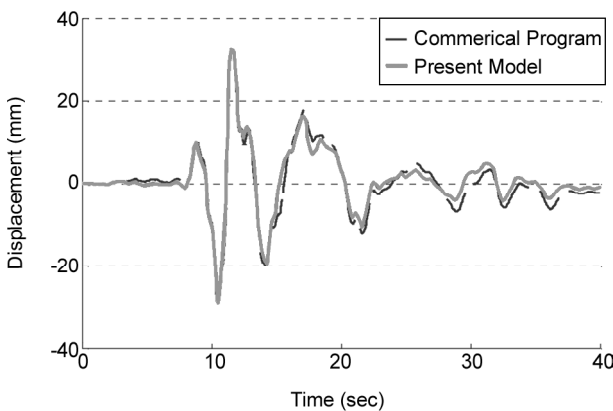


Figure 4. Results of the present model compared with that of a commercial program.

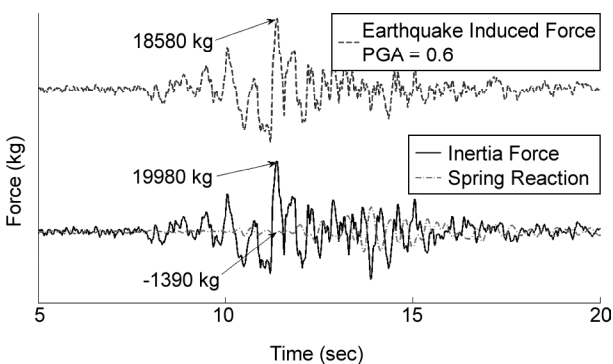


Figure 5. Contribution of inertia force and support reaction.

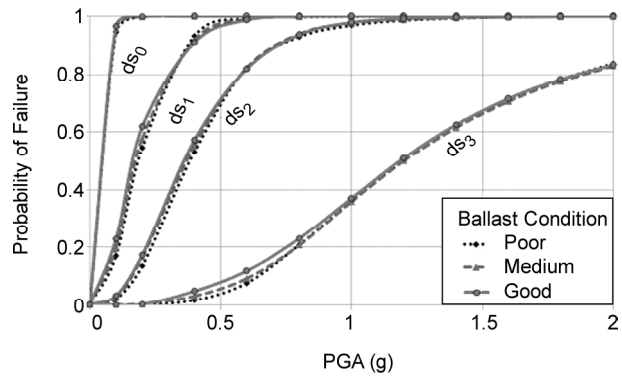


Figure 6. Fragility curves for track with concrete ties (Damage level: ds_0 = none, ds_1 = minor, ds_2 = moderate, ds_3 = Complete).

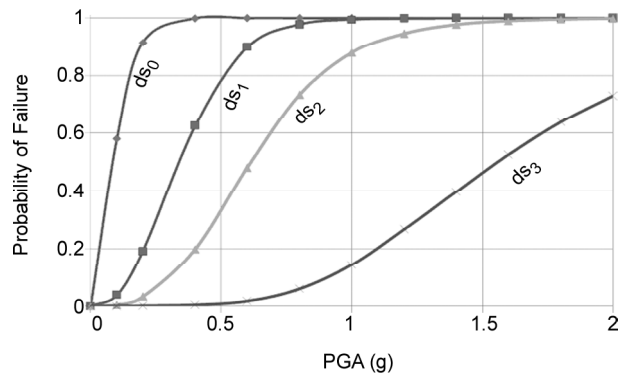


Figure 7. Fragility curves for track with wood ties (Damage level: ds_0 = none, ds_1 = minor, ds_2 = moderate, ds_3 = Complete).

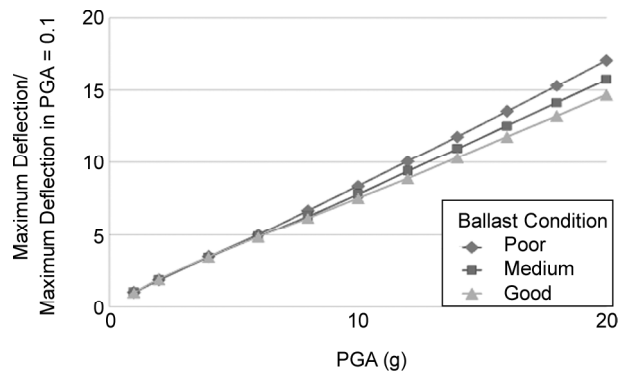


Figure 8. Ratio of the maximum lateral deflection of the track to the maximum deflection at PGA = 0.1 g.

In modeling the track system, a parameter κ is used to represent the level of fastener rigidity. κ varies from zero, for no rigidity, to one, for complete rigidity. The results of Figures (6) and (7) are based on zero rigidity. For complete rigidity, the maximum deflection decreases by about 5 percent. For UIC54 and 143.5 cm gauge the moment of inertia of the track increases from 834 cm⁴, for $\kappa=0$ to 782267 cm⁴, for $\kappa=1$. The lateral stiffness of the system is 938 times greater than that for connection with no rigidity. In seismic analysis, in addition to the spring forces, inertia forces are acting against the motion. The maximum deflection of railroad tracks is not too sensitive to changing stiffness of their components, such as ballast consolidation, moment of inertia of the rail and quality of fasteners. Therefore, the best way to reduce the effect of earthquakes and prevent damage is to lighten the system. Since a major portion of the weight of the system is that of the ties, using wood ties instead of concrete can reduce the deformation of the system substantially.

10. Conclusions

In this study, nonlinear time history analysis has been used to determine the maximum deflection of the railroad system. An analytical method has been utilized for constructing fragility curves for assessment of seismic vulnerability. The influence of major parameters of the track on fragility curves has been investigated by considering three different foundation yield stresses and fastener rigidities and two different types of tie (wood and concrete). The results show that:

- ❖ Improved quality of ballast, going from poor to good, does not have an appreciable influence on the results.
- ❖ A change in the stiffness of the connection does not appear to have a significant effect on the results.
- ❖ A reduction of the weight of ties results in decreased earthquake forces.

References

1. Padgett, J. and DesRoches, R. (2008). Methodology for the Development of Analytical Fragility Curves for Retrofitted Bridges, *Earthquake Engineering and Structural Dynamics*, **37**, 1157-1174.
2. Basoz, N. and Kiremidjian, A.S. (1999). Development of Empirical Fragility Curves for Bridges, Technical Council on Lifeline Earthquake Engineering Monograph Proceedings of the 1999 5th U.S. Conference on Lifeline Earthquake.
3. Shinozuka, M., Feng, M.Q., Lee, J., and Naganuma, T. (2000). Statistical Analysis of Fragility Curves, *Journal of Engineering Mechanics*, **126**, 1224.
4. Yamazaki, F., Hamada, T., Motoyama, H., and Yamauchi, H. (1999). Earthquake Damage Assessment of Expressway Bridges in Japan, Technical Council on Lifeline Earthquake Engineering Monograph, 361-370.
5. Hwang, H., Jernigan, J., and Lin, Y-W. (2000). Evaluation of Seismic Damage to Memphis Bridges and Highway Systems, *Journal of Bridge Engineering*, **5**, 322-330.
6. Elnashai, A.S., Borzi, B., and Vlachos, S. (2004). Deformation-Based Vulnerability Functions for RC Bridges, *Structural Engineering and Mechanics*, **17**, 215-244.
7. Byers, W. (2004). Railroad Lifeline Damage in Earthquakes, *Proc. 13th World Conference on Earthquake Engineering*, Vancouver, B.C., Canada, Paper No.324.
8. Argyroudis, S. (2010). Contribution to Seismic Vulnerability and Risk of Transportation Networks in Urban Environment, PhD Thesis (in Greek), Dept. of Civil Engineering, and Aristotle University of Thessaloniki, Greece.
9. National Institute of Building Sciences (NIBS) (2004). HAZUS-MH: User's Manual and Technical Manuals, Report prepared for the Federal Emergency Management Agency, Washington, D.C.
10. Samavedam, G, Kish, A., and Jeong, D. (1983). Parametric Studies on Lateral Stability of Welded Rail Track, DOT, FRA-ORD-93/26, Washington, D.C., USA.
11. SAC Joint Venture Steel Project Phase 2, Develop Suites of Time Histories, Draft Report (1997). Published by the Federal Emergency Management Agency, FEMA-356, Washington, D.C.

12. McGuire, R.K. (1995). Probabilistic Seismic Hazard Analysis and Design: Closing the Loop, *Bull. Seismic Soc. Am.*, **86**, 1275-1284.
13. Kyriazis, P. (2011). Systemic Seismic Vulnerability and Risk Analysis for Buildings, Lifeline networks and Infrastructures Safety Gain, Project Title: Fragility Functions for Railway System Elements.
14. Arbabi, F. and Li, F. (1988). Effect of Nonlinear Parameters on Stresses in Railroad Tracks, *Journal of Structural Engineering*, **114**, 165-183.
15. Bazant, Z.P. and Cedolin, L. (1991). *Stability of Structures*, Oxford University Press, 373-380.
16. Murray, D.W. and Rajaserkaran, S. (1975). Technique for Formulation of the Beam Equations, *J. Engr. Mech. Div., ASCE*, **101**(5), 561-573.
17. WU, J.S. and SHIH, P.Y. (1999). The Dynamic Behavior of a Finite Railway under the High-Speed Multiple Moving Forces, Technique Report, Department of Naval Architecture and Marine Engineering, National Cheng-Kung University, Tainan, Taiwan. 701, R.O.C.
18. Samavedam, G., Blader, F., and Thomson, D. (1995). Track Lateral Shift: Fundamentals and State of-the-Art Review, Final Report, DOT/FRNORD.
19. Lichtberger, B. (2007). The Lateral Resistance of the Track, *European Railway Review*, Issue 3 & 4.
20. Samavedam, G., Kanaan, A., Pietrak, J., Kish, A., and Sluz, A. (1995). Wood Tie Track Resistance Characterization and Correlations Study, DOT/FRA/ORD-94/07, Final Report.
21. Kish, A., Clark, D.W., and Thompson, W. (1995). Recent Investigations on the Lateral Stability of Wood and Concrete Tie Tracks, *AREA Bulletin* 752, 96.
22. Naeim, F., Alimoradi, A., and Pezeshk, S. (2004). Selection and Scaling of Ground Motion Time Histories for Structural Design Using Genetic Algorithms, *Earthquake Spectra*, **20**(2), 413-426.
23. Kalkan, E. and Chopra, A.K. (2010). Practical Guidelines to Select and Scale Earthquake Records for Nonlinear Response History Analysis of Structures, U.S. Geological Survey Open-File Report, 113.
24. Ellingwood, B.R. (2001). Earthquake Risk Assessment of Building Structures, *Reliability Engineering and System Safety*, **74**(3), 251-262.
25. Cornell, A.C., Jalayer, F., and Hamburger, R.O. (2002). Probabilistic Basis for SAC Federal Emergency Management Agency Steel Moment Frame Guidelines, *Journal of Structural Engineering*, **128**, 526-532.
26. Kyriazis, P. (2011). Systemic Seismic Vulnerability and Risk Analysis for Buildings, Lifeline Networks and Infrastructures Safety Gain, Efficient, Intensity Measures for Components within a Number of Infrastructures, Aristotle University of Thessaloniki.
27. Argyroudis, S., Monge, O., Finazzi, D., and Pessina, V. (2003). Vulnerability Assessment of Lifelines and Essential Facilities (WP06), Methodological Handbook - Appendix 1: Roadway Transportation System, Risk-UE Final Report, Report n° GTR-RSK 0101-152av7.
28. Kyriazis, P. (2011). Systemic Seismic Vulnerability and Risk Analysis for Buildings, Lifeline Networks and Infrastructures Safety Gain, Fragility Functions for Roadway System Elements.
29. Housner, G.W. (1956). Earthquake-Resistant Design Based on Dynamic Properties of Earthquakes, *Journal of the American Concrete Institute*, **28**(1), Proceedings V. 53, 85-98.
30. Newmark, N.M. and Rosenblueth, E. (1971). *Fundamentals of Earthquake Engineering*, Prentice-Hall, Inc., Englewood Cliffs, N.J.
31. SAP2000 (1995). Computer and Structures, Inc. 1995 University Avenue Berkeley, California 94704 USA.

Appendix I

Matrix relating global to local displacements:

$$D = \begin{bmatrix} f_1' & \cdot & \cdot & \cdot & \cdot & \cdot & \cdot \\ \cdot & f_3'' & \cdot & \cdot & \cdot & f_4'' & \cdot \\ \cdot & \cdot & f_3'' & \cdot & -f_4'' & \cdot & \cdot \\ \cdot & \cdot & \cdot & f_3' & \cdot & \cdot & f_4' \end{bmatrix}$$

$$\left[\begin{array}{cccccc} f_2' & \cdot & \cdot & \cdot & \cdot & \cdot \\ \cdot & f_5'' & \cdot & \cdot & \cdot & f_6'' \\ \cdot & \cdot & f_5'' & \cdot & -f_6'' & \cdot \\ \cdot & \cdot & \cdot & f_5' & \cdot & f_6' \end{array} \right]$$

Matrix of shape functions:

$$F = \begin{bmatrix} f_1 & \cdot & \cdot & \cdot & \cdot & \cdot \\ \cdot & f_3 & \cdot & \cdot & \cdot & f_4 \\ \cdot & \cdot & f_3 & \cdot & -f_4 & \cdot \\ \cdot & \cdot & \cdot & f_3 & \cdot & f_4 \end{bmatrix}$$

$$\left[\begin{array}{cccccc} f_2 & \cdot & \cdot & \cdot & \cdot & \cdot \\ \cdot & f_5 & \cdot & \cdot & \cdot & f_6 \\ \cdot & \cdot & f_5 & \cdot & -f_6 & \cdot \\ \cdot & \cdot & \cdot & f_5 & \cdot & f_6 \end{array} \right]$$

$$f_1 = 1 - \xi, f_2 = \xi, f_3 = 1 - 3\xi^2 + 2\xi^3,$$

$$f_4 = (\xi - 2\xi^2 + \xi^3)l, f_5 = 3\xi^2 - 2\xi^3,$$

$$f_6 = (\xi^3 - \xi^3)l, \xi = x/l$$

Stiffness matrix for the support system:

$$\mathbf{K}_s = \begin{bmatrix} \mathbf{K}_{s_1} & \cdot \\ \cdot & \mathbf{K}_{s_2} \end{bmatrix}. \text{ Sub matrices } \mathbf{K}_{s_i}, i = 1, 2 \text{ are}$$

defined as

$$\mathbf{K}_{s_i} = \begin{bmatrix} \lambda_{u_i} & \cdot & \cdot & \cdot & \cdot & \cdot & \cdot \\ \cdot & \lambda_{v_i} & \cdot & -\lambda_{v_i} h_z & \cdot & \cdot & \cdot \\ \cdot & \cdot & \lambda_{w_i} & \lambda_{w_i} h_y & \cdot & \cdot & \cdot \\ \cdot & -\lambda_{v_i} h_z & \lambda_{w_i} h_y & \lambda_{\theta_i}^* & \cdot & \cdot & \cdot \\ \cdot & \cdot & \cdot & \cdot & \lambda_{\theta_{y_i}} & \cdot & \cdot \\ \cdot & \cdot & \cdot & \cdot & \cdot & \lambda_{\theta_{z_i}} & \cdot \\ \cdot & \cdot & \cdot & \cdot & \cdot & \cdot & \lambda_{\omega} \end{bmatrix}$$

$$\lambda_{\theta_i}^* = \lambda_v h_z + \lambda_z h_y + \lambda_{\theta_x}$$

λ_u, λ_v and λ_w are longitudinal, vertical and lateral spring stiffness and $\lambda_{\theta_x}, \lambda_{\theta_y}$ and λ_{θ_z} are rotational spring stiffness about x-, y- and z- axes, respectively. λ_{ω} is the warping spring constant.

Nomenclature

- a_0, a_1 = Constants related to stiffness and mass matrices
- A = Cross-sectional area
- C = Damping matrix
- C = Capacity of a structure
- \mathbf{d} = Deformation gradient vector
- d = Half-distance between two rails
- d_s = Damage state
- D = Seismic demand
- E = Elasticity matrix
- E = Young's modulus
- F = Matrix of shape functions
- F_e = Limit of elastic resistance
- F_p = Peak resistance of ballast
- G = Shear modulus
- h_y, h_z = Distances in z- and y- directions from the shear center
- IM = Intensity measure
- I_p = Polar moment of inertia
- I_y, I_z = Area moment of inertia about y- and z- axes
- $\mathbf{K}_e, \mathbf{K}_{rail}$ = Stiffness matrix of rail element
- $\mathbf{K}_s, \mathbf{K}_{spring1}$ = Stiffness matrix of springs
- k_z = Spring constant in z- direction
- L = Length of element
- m = Mass per unit length
- $\mathbf{M}_r, \mathbf{M}_{rail}$ = Mass matrix of rail element
- \mathbf{M}_{tie} = Mass matrix of tie
- P_f = Probability of failure
- \mathbf{r} = Joint displacement vector
- r = Radius of gyration
- \mathbf{s} = Displacement vector
- S_{mi} = Median value of seismic demand
- T = Kinetic energy of rail element
- u_c = Displacement of centroid
- U_r, U_s = Elastic energy of deformation of rail and springs
- \mathbf{U} = Deformation vector
- v_s, w_s = Vertical and lateral displacements of shear center
- u, v, w = Displacement components of an arbitrary

point of rail element

V = Volume of rail element

W_e = Elastic displacement of ballast

W_p = Displacement of ballast at peak resistance

y_s, z_s = Coordinates of shear center

β_{DIM} = Logarithmic standard deviation at given seismic intensity level

ε_x = Normal strain

$\varepsilon_{xy}, \varepsilon_{xz}$ = Shear strains

$\boldsymbol{\varepsilon}$ = Strain tensor

ϕ = Axial rotation of rail section

Φ = Probability of exceeding a particular damage state

κ = Constant related to rigidity of fasteners

$\lambda_u, \lambda_v, \lambda_w$ = Longitudinal, vertical and lateral stiffness of springs

$\lambda_{\theta_x}, \lambda_{\theta_y}, \lambda_{\theta_z}$ = Rotational spring stiffness about x -, y - and z - axes

μ_f = Tie-ballast friction coefficient

σ_x = Normal stress

$\boldsymbol{\sigma}$ = Stress tensor

τ_{xy}, τ_{xz} = Shear stress